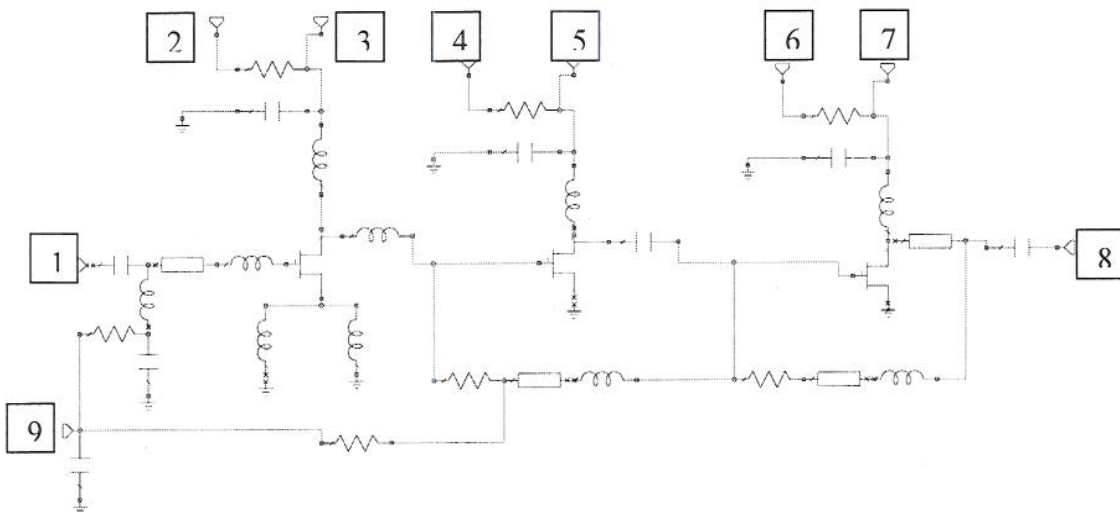


The Solutions for E4.18, 2008

Model answer to Q 1(a): Bookwork and Discussions in Class



This is a three-stage low noise amplifier with parallel feedback in the last two stages.

[10]

Model answer to Q 1(b): Bookwork and Discussions in Class

This amplifier used metal-semiconductor field-effect transistor (MESFET) technologies. This is the workhorse of microwave GaAs ICs. They have good general performance in gain, power-added efficiency, output power and noise. However, they do not have superior performance over HEMT devices. The inductors are all of the planar 2D spiral type. This gives high inductance per unit area but poor noise and bandwidth performance. The capacitors are all of the metal-insulator-metal type. These can give high capacitance values per unit area, but are prone to low yield due to pinhole short circuits.

Most MMIC devices have to be tailored to volume production and tend not to give state-of-the-art performance. This introduces compromises for the MMIC designer: (i) this can be a serious problem for LNA and PA design; (ii) special devices (e.g. Gunn diodes, PIN switches, and hyperabrupt varactor diodes) are rarely used in MMIC processes; (iii) FET switch is a poor substitute for the PIN diode and the HEMT millimetre-wave; (iv) oscillator will have a low output power compared with a Gunn diode; (v) most compromises can be absorbed into the specifications of the system design, and good communications between the circuit designer and systems designer are very beneficial to the final product.

[5]

Model answer to Q 1(c): Bookwork and Discussions in Class

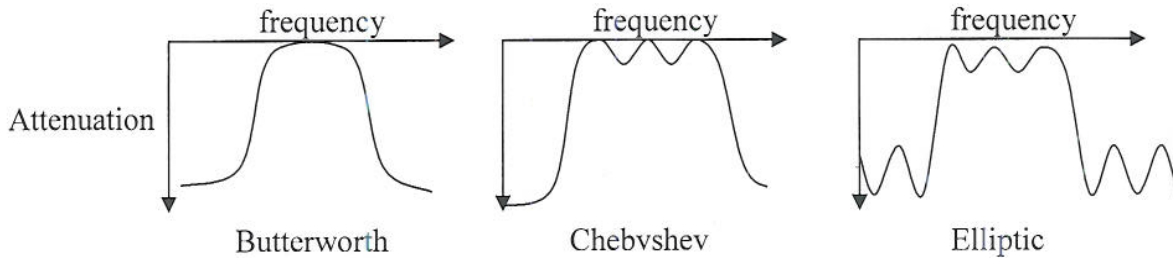
In practice, most of the components identified in 1(a) should be represented by many equivalent circuit model elements. As a result, while there are only 3 MESFETs, 8 capacitors, 10 spiral inductors, 7 resistors, 4 microstrip interconnections identified, the circuit could be represented by hundreds of individual parasitic elements. In order to reduce the chip size the components have to be placed closer together. However, by doing this, the electromagnetic coupling between components causes adverse interactions that can only be modelled sufficiently using 3D electromagnetics simulation packages.

[5]

Model answer to Q 2(a): Bookwork and Discussions in Class

Butterworth filters have a maximally flat frequency response in the passband. Chebyshev filters exhibit ripples in the passband only; the number depends on the filter order. Neither the Butterworth nor Chebyshev filters have ripples in the stopband. Elliptical filters have the sharpest roll-off attenuation characteristics of all three types, with the Chebyshev having sharper roll-off than the Butterworth. The elliptic filter exhibits ripples in the stopband (transmission zeros) as well as ripples in the passband (transmission poles).

Chebyshev and elliptic filters have higher group delays than the Butterworth, particularly near the 3 dB cut-off frequency and should be avoided in applications where pulse distortion is critical.



[5]

Model answer to Q 2(b): Computed Example

Determine $f/f_c = B/BW_{STOP} = 2$.

From curves: Butterworth with 0.00 dB ripples need $>7^{\text{th}}$ order.

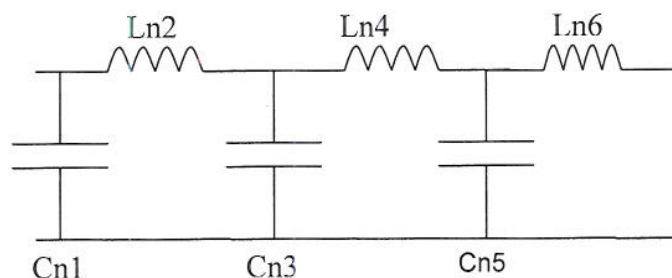
Chebyshev with 0.01 dB ripples need 6^{th} order for 46 dB rejection having $f/f_c = 2$.

Chebyshev with 0.10 dB ripples need 6^{th} order for 50 dB rejection having $f/f_c = 2$.

This last option is best, as it has good out-of-band attenuation margin.

For $R_{in}/R_{out} = R_s/R_L = 2$, the normalised prototype low pass filter coefficients are:

| Cn1 | Ln2 | Cn3 | Ln4 | Cn5 | Ln6 |
|-------|-------|-------|-------|-------|-------|
| 0.414 | 3.068 | 0.958 | 3.712 | 0.979 | 2.794 |



To de-normalize shunt capacitors and inductors:

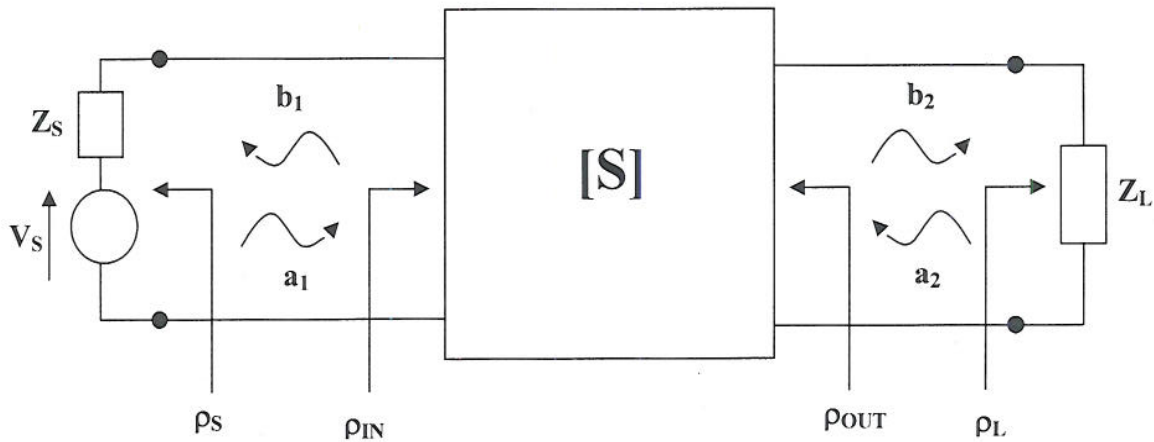
$$C_p = \frac{C_n}{2\pi f_c R_L} \quad L_p = \frac{R_L B}{2\pi f_c^2 C_n}$$

To de-normalize series inductors and capacitors:

$$L_s = \frac{L_n R_L}{2\pi B} \quad C_s = \frac{B}{2\pi f_o^2 L_n R_L}$$

| | |
|----------------|-----------------|
| Cp1 = 26.36 pF | Lp1 = 3.84 nH |
| Cs2 = 0.21 pF | Ls2 = 488.29 nH |
| Cp3 = 61.00 pF | Lp3 = 1.66 nH |
| Cs4 = 0.71 pF | Ls4 = 590.78 nH |
| Cp5 = 62.33 pF | Lp5 = 1.63 nH |
| Cs6 = 0.23 pF | Ls6 = 444.68 nH |

Model answer to Q 3(a): Bookwork



$$\text{Incident Wave, } a = \frac{V_+}{\sqrt{Z_0}} = \frac{1}{2} \left(\frac{V(0)}{\sqrt{Z_0}} + I(0)\sqrt{Z_0} \right) \equiv +I_+ \sqrt{Z_0}$$

$$\text{Reflected Wave, } b = \frac{V_-}{\sqrt{Z_0}} = \frac{1}{2} \left(\frac{V(0)}{\sqrt{Z_0}} - I(0)\sqrt{Z_0} \right) \equiv -I_- \sqrt{Z_0}$$

$$\text{therefore, } V(0) = \sqrt{Z_0}(a+b) \equiv (V_+ + V_-) \quad \text{and} \quad I(0) = \frac{(a-b)}{\sqrt{Z_0}} \equiv (I_+ + I_-)$$

$$\text{Power Incident At Port, } P_+ = |a|^2$$

$$\text{Power Reflected By Port, } P_- = |b|^2 = |\rho|^2 |a|^2$$

$$\text{Power Delivered to Port Termination Impedance, } P = (P_+ - P_-) = (|a|^2 - |b|^2) = |a|^2 (1 - |\rho|^2)$$

$$\text{Input Voltage Wave Reflection Coefficient, } S_{11} = \frac{b_1}{a_1} \bigg|_{a_2=0}$$

$$\text{Forward Voltage Wave Transmission Coefficient, } S_{21} = \frac{b_2}{a_1} \bigg|_{a_2=0}$$

$$\text{Insertion Phase} = \angle S_{21}$$

Reverse Voltage Wave Transmission Coefficient, $S_{12} = \frac{b_1}{a_2} \Big|_{a_1=0}$

Output Voltage Wave Reflection Coefficient, $S_{22} = \frac{b_2}{a_2} \Big|_{a_1=0}$

Input Return Loss, $RL_{IN} = 10 \log |S_{11}|^2$

**Insertion Power Gain (Loss), G_I
Forward Transducer Power Gain (Loss), G_{FT} } = $10 \log |S_{21}|^2$ when $Z_S = Z_L = Z_0$**

**Reverse Power Isolation, IS
Reverse Transducer Power Gain (Loss), G_{RT} } = $10 \log |S_{12}|^2$ when $Z_S = Z_L = Z_0$**

Output Return Loss, $RL_{OUT} = 10 \log |S_{22}|^2$

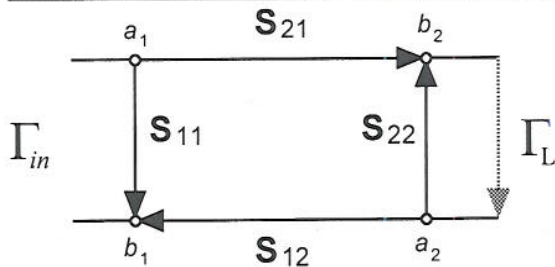
[5]

Model answer to Q 3(b): Computed Example

- (i) This is a lossless transmission line of length $2\lambda_g$, with perfect impedance matching to the reference impedance.
- (ii) This is an isolator. The insertion loss in the forward direction is 0 dB and 23.1 dB in the reverse direction. Again, perfect port impedance matching is achieved.
- (iii) This is an amplifier with forward power gain of 19.7 dB, reverse isolation of 10.45 dB. If the output is matched, the input return loss is 20 dB. If the input is matched, the output return loss is 16.5 dB.

[5]

Model answer to Q 3(c): Textbook Example



$$\begin{aligned}
 b_1 &= S_{11}a_1 + S_{12}(\Gamma_L b_2) \\
 b_2 &= S_{21}a_1 + S_{22}(\Gamma_L b_2) \\
 \therefore b_2 &= (1 - \Gamma_L S_{22}) = S_{21}a_1 \\
 \therefore \Gamma_{in} &= S_{11} + \frac{S_{21}S_{12}\Gamma_L}{1 - S_{22}\Gamma_L}
 \end{aligned}$$

[6]

Model answer to Q 3(d): Textbook Example

If $|\Gamma_{in}| \leq 1$, the circuit will be unconditionally stable. Since $S_{11} = S_{22} = 0$, $|\Gamma_{in}| \leq S_{21}S_{12} = 0.07e^{-j\pi/2}$ and $|\Gamma_{in}| = 0.07/2 \ll 1$, i.e. unconditionally stable!

[4]

Model answer to Q 4: Computed Example

| | | | | | | |
|------------------------|------|-----|-------|-------|-------|-----|
| | | | | | | |
| | | | | | | |
| G [dB] | | +15 | +8 | +4 | -0.7 | |
| IP ₃ [dBm] | | +30 | +40 | +50 | | |
| F [dB] | | +1 | +2 | +3 | | |
| | | | | | | |
| P _{out} [dBm] | +3 | +18 | +26 | +30 | +29.3 | [2] |
| IP ₃ [dBm] | | +30 | +35.9 | +39.5 | +38.8 | [6] |
| IMD ₃ [dBc] | | +24 | +19.8 | +19 | +19 | [3] |
| I ₃ [dBm] | | -6 | +6.2 | +11 | +10.3 | [3] |
| F [dB] | +1.1 | | | | | [6] |

Using the following general equations:

$$C = P_{OUT}(f_0) = G_1 G_2 P_{IN} \quad \text{and} \quad IP_3 = (IP_3|_1 G_2) \| IP_3|_2$$

$$IMD_3 = \frac{C}{I_3} \sim \left(\frac{IP_3}{C} \right)^2 \equiv 2(IP_3[dBm] - C[dBm])[dBc]$$

$$F = F_1 + \frac{F_2 - 1}{G_1} + \frac{F_3 - 1}{G_1 G_2} + \frac{F_4 - 1}{G_1 G_2 G_3} + \dots$$

Model answer to Q 5(a): Bookwork

Designing high-performance narrow fractional bandwidth filters is more difficult than designing for wider bandwidths. The reason is that more components are needed to get steeper roll-off characteristics. As a result, energy stays within the filter for longer and so the group delay of the filter increases. Moreover, the longer the energy stays within the filter the more of it will be dissipated as unwanted heat and so the pass-band attenuation increases. For this reason, the components must increase in size, in order to reduce current densities and, thus, reduce the associated wasted power dissipated within the components' materials. Therefore, using passive realization technologies, narrow fractional bandwidth filters have to be relatively large.

[4]

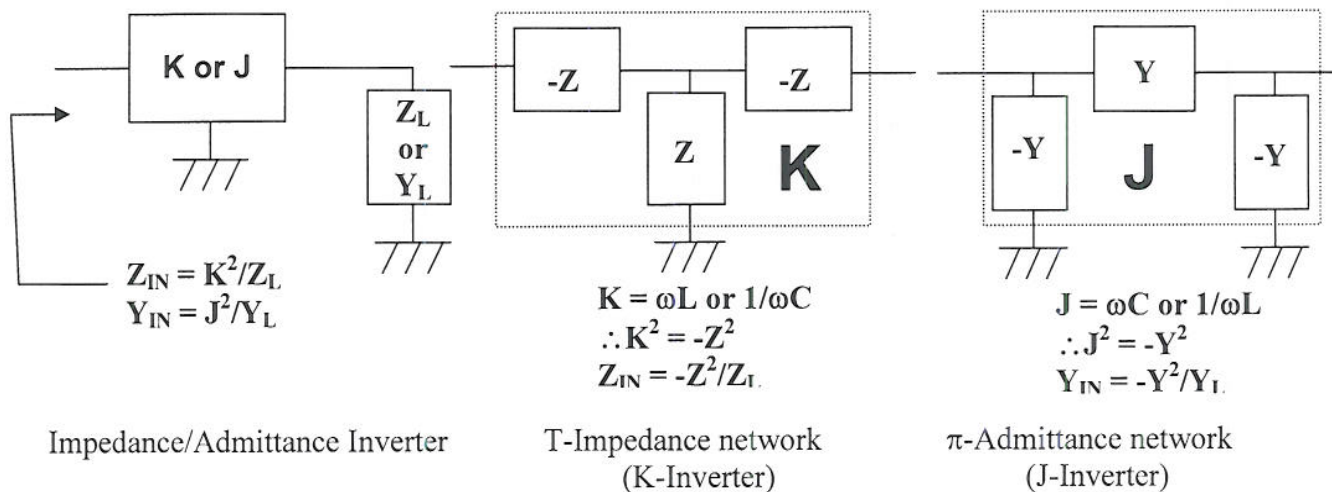
Model answer to Q 5(b): Bookwork

In addition to size, as the fractional bandwidth of a filter gets smaller, the required range of L and C components values increases. In practice, it may not be possible to achieve such a high range from a discrete component. For this reason, impedance and/or admittance inverters are used to convert the component values that are available into those that are not normally available. It has already been shown that a $\lambda g/4$ section of transmission line can be used to perform impedance inversion:

$$Z_{IN} = K^2/Z_L \quad \text{Impedance inversion constant, } K = Z_0 \text{ with } \lambda g/4 \text{ transmission line}$$

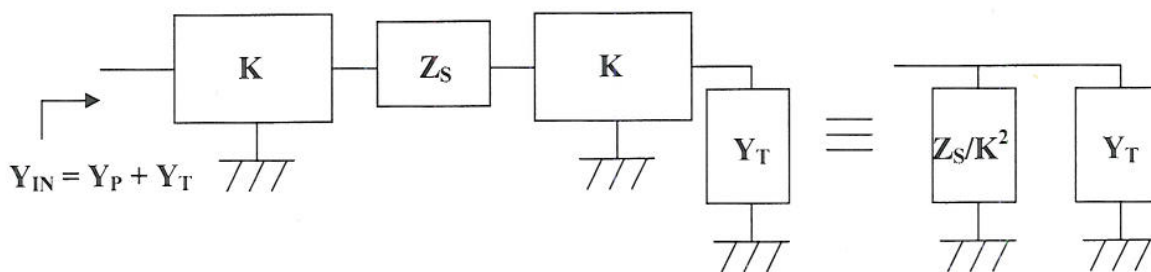
$$Y_{IN} = J^2/Y_L \quad \text{Admittance inversion constant, } J = Y_0 \text{ with } \lambda g/4 \text{ transmission line}$$

In addition, lumped elements can be used (i.e. either all inductive or all capacitive), as shown below. Note that negative reactances or susceptances are meant to be absorbed by neighbouring positive reactances or susceptances.

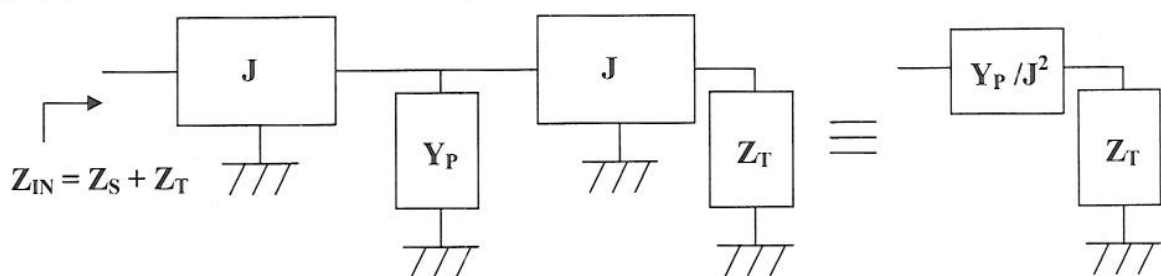


- Two identical inverters connected in cascade represents a zero inversion
- A series (shunt) element placed between two identical inverters appears as a shunt (series) element

As an example, a shunt connected parallel L-C tuned circuit can be “synthesized” from a series connected series L-C tuned circuit having two impedance inverters.



As an example, a series connected series L-C tuned circuit can be “synthesized” from a shunt connected parallel L-C tuned circuit having two admittance inverters.



[6]

Model answer to Q 5(c): Computed Example

A series R-L-C circuit has the following impedance:

$$Z_S = R_S + j\omega L_S + \frac{1}{j\omega C_S}$$

This can be converted into a shunted parallel R-L-C tuned circuit by using J-inverters. The corresponding admittance will be:

$$Y_p = G_p + j\omega C_p + \frac{1}{j\omega L_p} \equiv \frac{J^2}{Y_s} = Z_s J^2$$

Using discrete capacitance values to realise an admittance inverter with a $-C/+C/-C$ π -network:

$$J = \omega C$$

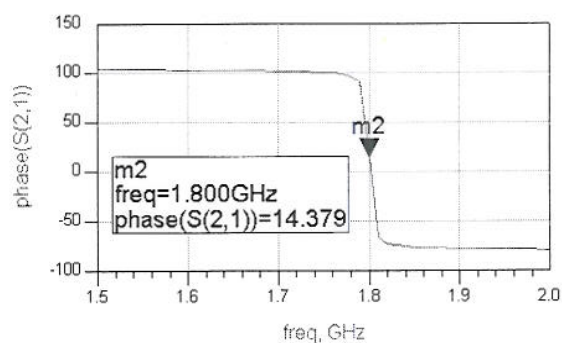
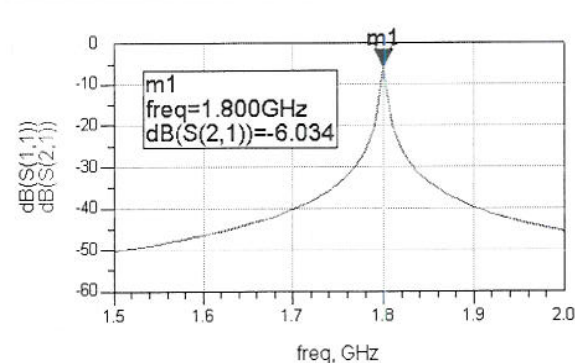
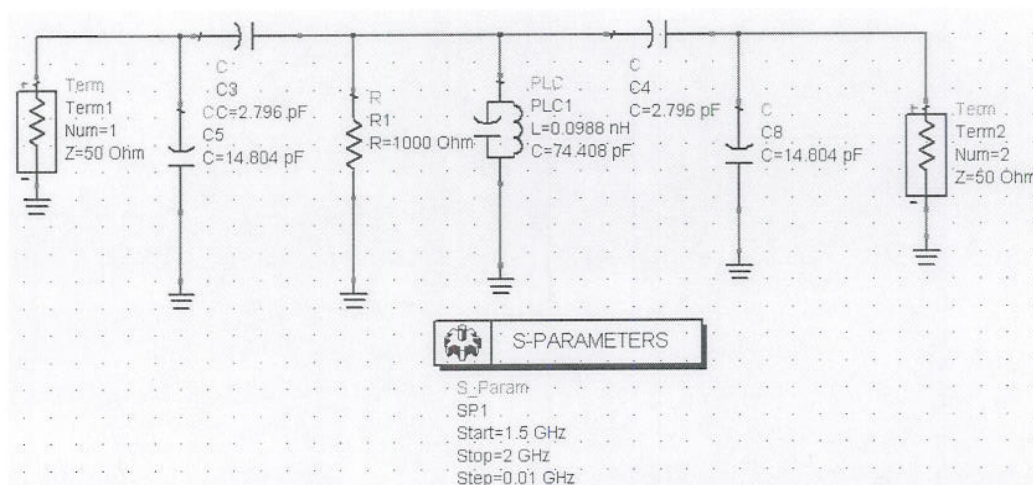
$$Y_p = R_s(\omega C)^2 + j\omega L_s(\omega C)^2 + \frac{(\omega C)^2}{j\omega C_s}$$

$$\therefore R_p = \frac{1}{R_s(\omega C)^2} \quad ; \quad C_p = L_s(\omega C)^2 \quad ; \quad L_p = \frac{C_s}{(\omega C)^2}$$

If we choose:

$$(\omega C)^2 = 1 \times 10^{-3} \quad \therefore C = 2.796 \text{ pF} \quad \text{for } f = 1.8 \text{ GHz}$$

$$\therefore R_p = 1,000 \, \Omega \quad ; \quad C_p = 80 \text{ pF} \quad ; \quad L_p = 0.0988 \text{ nH}$$



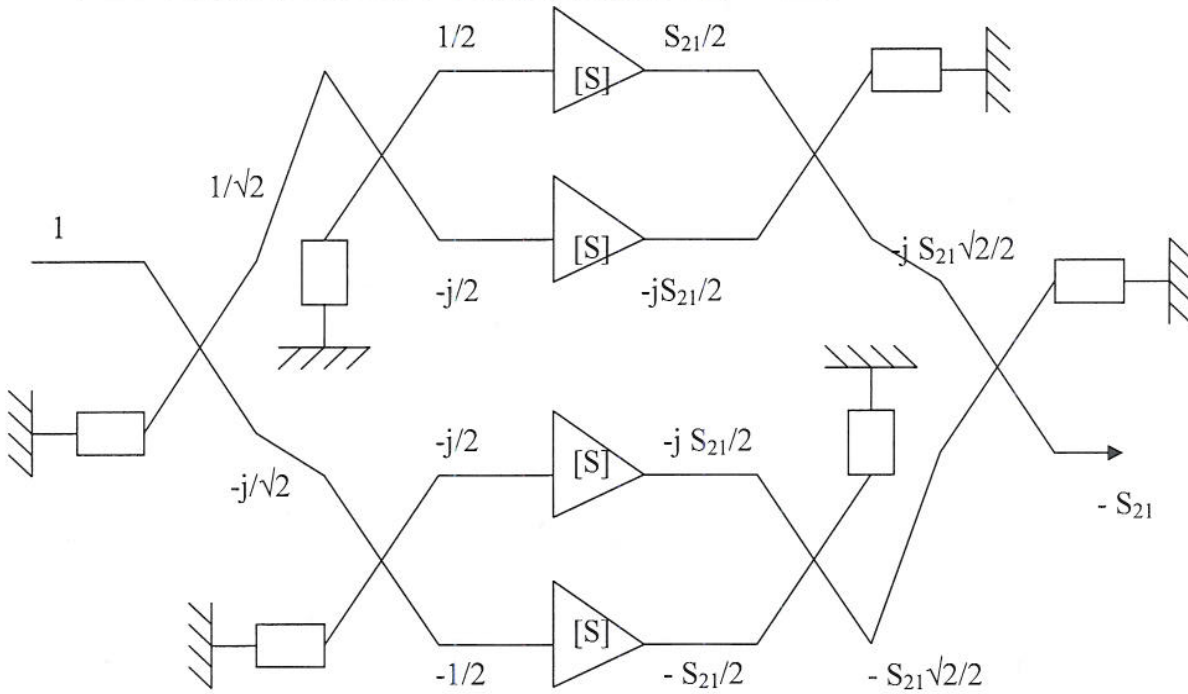
[8]

Model answer to Q 5(d): Extended Theory

Each J-inverter introduces 90° of insertion phase and, therefore, a pair of J-inverters will introduce 180° of insertion phase.

[2]

Model answer to Q 6(a): New application of theory



$$S_{21} |_{overall} = \left(\frac{1}{\sqrt{2}} \right) \left(\frac{1}{\sqrt{2}} \right) S_{21} \left(\frac{-j}{\sqrt{2}} \right) \left(\frac{-j}{\sqrt{2}} \right) + \left(\frac{1}{\sqrt{2}} \right) \left(\frac{-j}{\sqrt{2}} \right) S_{21} \left(\frac{-1}{\sqrt{2}} \right) \left(\frac{-j}{\sqrt{2}} \right) +$$

$$\left(\frac{-j}{\sqrt{2}} \right) \left(\frac{1}{\sqrt{2}} \right) S_{21} \left(\frac{-j}{\sqrt{2}} \right) \left(\frac{1}{\sqrt{2}} \right) + \left(\frac{-j}{\sqrt{2}} \right) \left(\frac{-j}{\sqrt{2}} \right) S_{21} \left(\frac{1}{\sqrt{2}} \right) \left(\frac{1}{\sqrt{2}} \right) = -S_{21}$$

$$Insertion Loss = 10 \log \{ |S_{21}|^2 \}$$

$$S_{11} |_{overall} = \left(\frac{1}{\sqrt{2}} \right) \left(\frac{1}{\sqrt{2}} \right) S_{11} \left(\frac{1}{\sqrt{2}} \right) \left(\frac{1}{\sqrt{2}} \right) + \left(\frac{1}{\sqrt{2}} \right) \left(\frac{-j}{\sqrt{2}} \right) S_{11} \left(\frac{-j}{\sqrt{2}} \right) \left(\frac{1}{\sqrt{2}} \right) +$$

$$\left(\frac{-j}{\sqrt{2}} \right) \left(\frac{1}{\sqrt{2}} \right) S_{11} \left(\frac{1}{\sqrt{2}} \right) \left(\frac{-j}{\sqrt{2}} \right) + \left(\frac{-j}{\sqrt{2}} \right) \left(\frac{-j}{\sqrt{2}} \right) S_{11} \left(\frac{-j}{\sqrt{2}} \right) \left(\frac{-j}{\sqrt{2}} \right) = 0$$

$$Return Loss = 10 \log \{ |0|^2 \} \rightarrow -\infty$$

[10]

Model answer to Q 6(b): Discussions in Class

The main application of this amplifier is power combining, since the output power is ideally a factor of 4 greater than that of the single-ended amplifier. If one of the single-ended amplifiers fails then $S_{21}|_{overall} = 3S_{21}/4$ and Insertion loss is $10 \log \{ (3|S_{21}|/4)^2 \} = 17.5 \text{ dB}$, i.e. a drop of 2.5 dB from a fully working amplifier. The input return loss should not change if the impedance of the failed amplifier doesn't change and is, therefore, still minus infinity. Therefore, this type of power combining amplifier is useful because it provides redundancy in the case of failure and also ideal port impedance matching. The disadvantages of this topology is that it requires 4 identical single-ended amplifiers. Also, practical losses in the couplers result in a direct loss in power gain and output efficiency will be significantly reduced.

[10]